RESEARCH ARTICLE
10.1002/2014JA020822

On the onset of ionospheric precursors 40 min before strong earthquakes

F. Masci[1], J. N. Thomas[2,3,4], F. Villani[1], J. A. Secan[2], and N. Rivera[3]

[1]Istituto Nazionale di Geofisica e Vulcanologia, L'Aquila, Italy, [2]NorthWest Research Associates, Redmond, Washington, USA, [3]Department of Electrical and Computer Engineering, DigiPen Institute of Technology, Redmond, Washington, USA, [4]Department of Earth and Space Sciences, University of Washington, Seattle, Washington, USA

Abstract Heki (2011) and Heki and Enomoto (2013) claimed that anomalous, yet similar, increases of ionospheric total electron content (TEC) started ~40 min prior to the 2011 Tohoku-Oki, as well as before other $M_w > 8$ earthquakes. The authors concluded that the reported TEC anomalies were likely related to the pending earthquakes, suggesting also that TEC monitoring may be useful for future earthquake prediction. Here we carefully examine the findings of Heki (2011) and Heki and Enomoto (2013) by performing new analyses of the same TEC data. Our interpretation is that the 40 min onset of the ionospheric precursors is an artifact induced by the definition of the reference line adopted in analyzing TEC variations. We also discuss this repeatability in the tectonic and geodynamic context of the earthquakes. By performing a Superimposed Epoch Analysis of TEC data, we show that, however, the TEC increase reported by Heki (2011) was not particularly anomalous. We conclude that the TEC precursors reported by Heki (2011) and Heki and Enomoto (2013) are not useful for developing short-term earthquake prediction capabilities.

1. Introduction

Increases of the ionospheric total electron content (TEC) were recently reported just before strong earthquakes [see *Cahyadi and Heki*, 2013; *Heki*, 2011; *Heki and Enomoto*, 2013] including the 2011 Tohoku-Oki earthquake. The TEC enhancements were considered to be possibly linked to the preparatory phase of the pending earthquake.

The M_w 9.0 Tohoku-Oki, Japan, earthquake of 11 March 2011 05:46:23 UTC occurred under the Pacific Ocean approximately 70 km east of Honshu, Japan (38.32°N, 142.37°E). This earthquake was one of the largest earthquakes ever recorded by seismometers. The earthquake and the subsequent tsunami resulted in some 19,000 deaths and economic losses exceeding 200 billion U.S. dollars [*Kajitani et al.*, 2013]. There were several reports of magnetic and ionospheric perturbations near the time of the 2011 Tohoku-Oki earthquake, both coseismic [see *Astafyeva et al.*, 2011; *Hao et al.*, 2012, 2013; *Kakinami et al.*, 2012; *Maruyama and Shinagawa*, 2014; *Rolland et al.*, 2011; *Utada et al.*, 2011] and precursory [see *Heki*, 2011; *Le et al.*, 2013]. However, reports of earthquake precursory signals are controversial [see, e.g., *Campbell*, 2009; *Masci*, 2010, 2011; *Moldovan et al.*, 2012; *Thomas et al.*, 2009a, 2009b], and despite several published studies, the physical generation mechanisms of the reported anomalies are still unclear. Recently, some reviews [see *Masci*, 2012, 2013; *Masci and Thomas*, 2014; *Thomas et al.*, 2012a] have demonstrated that reported preearthquake ionospheric anomalies are not uniquely associated with seismic activity.

The ionosphere is subject to numerous influences such as solar activity, geomagnetic activity, meteorological events, and anthropogenic effects. It also shows normal seasonal, day-to-day, and diurnal variations. Thus, it is difficult to clearly identify possible preseismic ionospheric anomalies. Some researchers, by means of statistical studies, claimed to have found an anomalous TEC behavior within a few days prior to strong earthquakes suggesting also that they may be related to the pending earthquakes [see, e.g., *Le et al.*, 2011]. In contrast, other studies found preearthquake anomalous TEC changes but no statistically significant correlation between the TEC anomalies and seismic activity [see, e.g., *Dautermann et al.*, 2007]. Although these reports do not disprove the existence of precursory phenomena, they have shown that, even during periods of low solar and geomagnetic activity [*Astafyeva and Heki*, 2011], changes in preearthquake TEC may be linked to changes in solar and geomagnetic activity. These changes induce not only global alteration of the ionosphere but may also control changes of ionospheric parameters, such as TEC, on a regional scale [see *Afraimovich and Astafyeva*, 2008].

In a paper published in *Geophysical Research Letters*, *Heki* [2011] reported an anomalous STEC (slant TEC; measured in TEC units, where 1 TECU = 10^{16} electrons/m^2) increase starting about 40 min prior to the Tohoku-Oki earthquake [see *Heki*, 2011, Figure 2]. The author analyzed Global Positioning System (GPS) data from the Japanese Earth Observation Network (GEONET). GEONET includes more than 1000 continuous GPS stations. GPS satellite signals (1575.42 and 1227.60 MHz carrier phase frequencies) are transmitted to ground stations through the ionosphere, and the phase of these signals are affected by the path-integrated electron density known as slant TEC. The anomaly identified by *Heki* [2011] is relative to a cubic least squares fit to the STEC time series (see the supporting information, description of the method, in *Heki* [2011]). According to *Heki* [2011], $M_w > 8$ earthquakes are preceded by similar anomalous preseismic STEC increases. The TEC anomaly is followed by a coseismic ionospheric disturbance (CID). On the contrary, $M_w < 8$ earthquakes show CIDs but no evident precursory signal. CIDs are caused by the arrival of atmospheric waves excited by the vertical motion of the ground (or sea level) and usually appear within a few minutes after the earthquake [*Calais and Minster*, 1995]. Even if the CID is an ionospheric effect that occurs following the shock, hereinafter we refer to it either as coseismic and postseismic disturbance in the same way as previously published papers [see, e.g., *Astafyeva et al.*, 2011]. According to *Heki* [2011], his reported preearthquake anomaly is qualitatively different from other examples of precursors since the TEC increase is temporally and spatially correlated with the earthquake, and the amplitude shows dependence with the magnitude [see *Heki*, 2011, Figure 4]. *Heki* [2011] concluded that M_w 9 class earthquakes like Tohoku-Oki might be predicted by monitoring the ionosphere above the fault zone. Preseismic STEC changes similar to that of the 2011 Tohoku-Oki earthquake were also reported by *Cahyadi and Heki* [2013] at the time of the 2007 Bengkulu earthquake by using the same method adopted by *Heki* [2011].

Some researchers have cast doubt on the seismogenic origin of the preearthquake STEC increase documented by *Heki* [2011] before the Tohoku-Oki earthquake. *Thomas et al.* [2012b] and *Kamogawa and Kakinami* [2013] hypothesized that the STEC increase reported by *Heki* [2011] is an artifact due to the reference curve adopted in analyzing TEC variations rather than a precursor. In the interpretation of *Kamogawa and Kakinami* [2013], the TEC increase preceding the Tohoku-Oki earthquake was due to the combined effect of the following: (i) applying a cubic fit to a TEC time series that included a "tsunamigenic ionospheric hole" [see *Kakinami et al.,* 2012], that is, a wide TEC depletion occurred after the coseismic atmospheric wave generated by the main shock that reached and perturbed the ionosphere; and (ii) TEC changes induced by strong geomagnetic activity. *Astafyeva et al.* [2013] suggested an alternative interpretation of the TEC depletion that is observed after strong earthquakes. They hypothesized that the TEC "hole" represents the negative phase on an N-like shape wave, a compression-rarefaction wave generated by the earthquake that propagates upward through the atmosphere and, due to the exponential decrease of the air density, grows in amplitude by several orders of magnitude before perturbing the ionosphere. The two-dimensional atmosphere-ionosphere simulation of *Shinagawa et al.* [2013] supports the idea that the decrease of TEC a few minutes after the Tohoku-Oki earthquake was caused by the strong expansion of the thermosphere driven by the pressure pulse induced by the sudden coseismic vertical motion of the sea surface. All these studies do not support the hypothesis that the Tohoku-Oki earthquake was preceded by precursory TEC changes.

In a recent paper, *Heki and Enomoto* [2013] reported new analyses of GPS-TEC data. They examined vertical TEC (VTEC), instead of the STEC investigated by *Heki* [2011], at the time of four $M_w > 8$ earthquakes: the 2011 Tohoku-Oki earthquake, the 2007 Bengkulu earthquake (M_w 8.4), the 2012 North Sumatra earthquake (M_w 8.6), and its largest aftershock (M_w 8.2) that occurred ~2 h later. *Heki and Enomoto* [2013] concluded that VTEC time series shows a similar behavior for all of these earthquakes (see Figure 1). More precisely, (i) VTEC starts to increase ~40 min prior the occurrence of each earthquake; (ii) about 10 min after the main shock, a transient positive CID is clearly evident; and (iii) VTEC quickly recovers to the normal level a few tens of minutes later. According to them, the striking similarity of the VTEC before the four earthquakes, supported by magnetic and ionosonde data, reinforces the hypothesis that the preearthquake TEC increases have a seismogenic origin. This led *Heki and Enomoto* [2013] to hypothesize a possible implication of TEC monitoring for short-term earthquakes prediction. Since prediction of strong earthquakes is an important topic for science and society, we were motivated to examine the findings of *Heki* [2011] and *Heki and Enomoto* [2013].
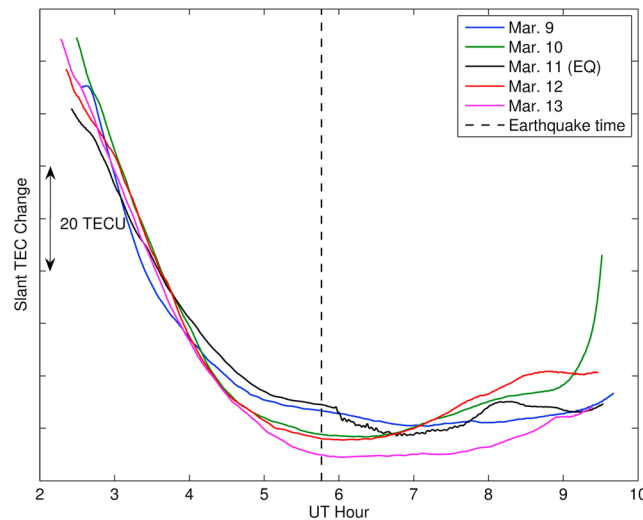
2. Our Own STEC Analysis

Heki [2011] reported STEC increases, relative to a cubic fit of the STEC time series, starting about 40 min prior to the Tohoku-Oki 2011 earthquake. Here we attempt to reproduce these results. We first calculate the STEC
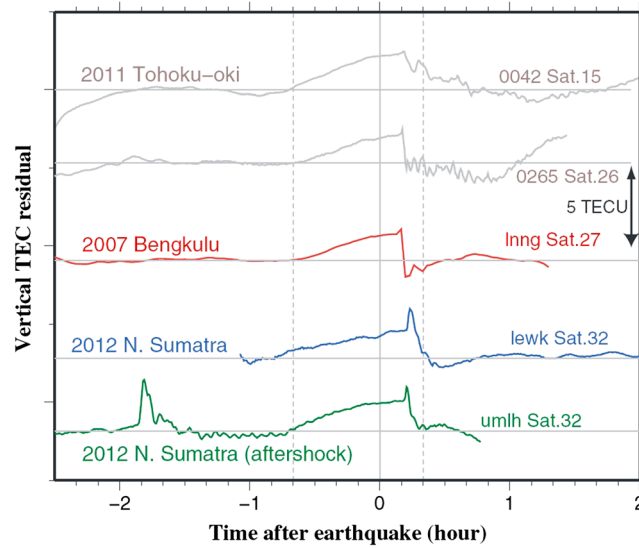
Figure 1. VTEC residuals as calculated by *Heki and Enomoto* [2013, Figure 8] for the 2011 Tohoku-Oki earthquake, the 2007 Bengkulu earthquake (M_w 8.4), the 2012 North Sumatra earthquake (M_w 8.6), and its largest aftershock (M_w 8.2) that occurred ~2 h later. The reference curves were defined by fitting the VTEC before and after the earthquake excluding the 1 h period between the two dashed vertical lines (−40 to +20 min centered at the earthquake time $t = 0$). Refer to *Heki and Enomoto* [2013] for details.

time series derived from 30 s GPS data [see *Bishop et al.,* 1994; *Mazzella et al.,* 2007] recorded at the same Japan GEONET stations as used by *Heki* [2011]. Figure 2 shows our STEC time series on 9–13 March 2011 for GEONET GPS station 3009 in Japan and satellite 015. *Heki* [2011] presented STEC from the same station-satellite pair in his Figure 2 and reported that the enhancement starting at approximately 5:00 UT 11 March is a possible precursor. Our STEC time series on 11 March (black curve) agrees with the results presented by *Heki* [2011], and a coseismic and/or tsunami-driven ionospheric disturbance is clearly seen starting a few minutes after the main shock. We note that the 11 March STEC time series is very similar to the 9 March time series (blue curve) and shows the same trend from 5:00 to 5:50 UT, the time of the possible precursor. The flattening of the STEC drop starting around 5:00 UT is normal and is seen on surrounding days; thus, the enhancement in the STEC time series on 11 March is not uniquely related to the earthquake occurrence.
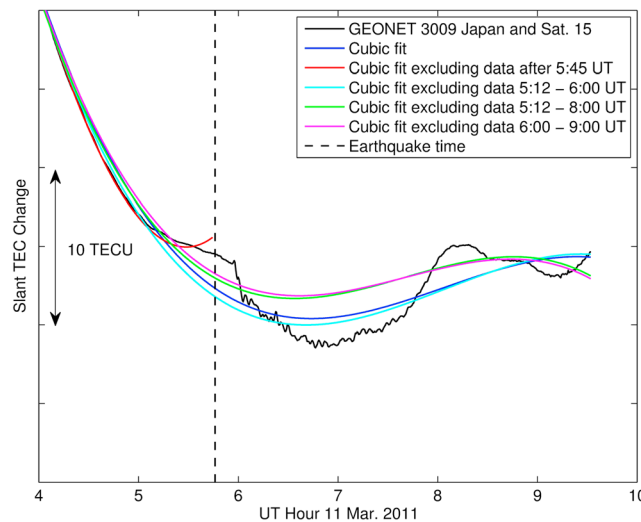
In Figure 3, we compare the STEC time series on the earthquake day for station 3009 and satellite 015 with modeled curves given by cubic least squares fits, which is the same method used by *Heki* [2011]. The blue curve uses the entire STEC time series, whereas the red curve excludes data from after 05:45 UT. The red curve shows that after removing the coseismic/tsunami disturbance, the cubic fit curve and the STEC time series are in strong agreement prior to the earthquake time. We note that *Heki* [2011] excluded data from 5:12 to 6:00 UT prior to applying a cubic fit, which he considered to be influenced by the preseismic TEC anomaly (see the supporting information, description of the method, in *Heki* [2011]). We follow this procedure as well, and this is shown as the cyan curve in Figure 3. In Figure 3, we also show cubic fit curves (green and magenta curves) that exclude data from the coseismic disturbance period, which highlights the sensitivity of the *Heki* [2011] fitting method to data exclusion. We find that including data from the coseismic disturbance after 6:00 UT biases the cubic fit curves (blue and

Figure 2. Slant TEC on 9–13 March 2011 for GEONET GPS station 3009 in Japan and satellite 15. The time of the earthquake (5:46 UT) on 11 March is shown as the black vertical dashed line. A coseismic ionospheric disturbance is clearly seen on 11 March (black curve) starting a few minutes after the earthquake. *Heki* [2011] reported that the enhancement of the slant TEC curve starting at 5:00 UT 11 March is a possible precursor. See text for details.

Figure 3. Slant TEC on 11 March 2011 for GEONET GPS Station 3009 in Japan and satellite 15. The time of the earthquake (5:46 UT) on 11 March is shown as the black vertical dashed line. Cubic least squares fits to the slant TEC with and without the preseismic and coseismic disturbance are shown. See text for details.

cyan curves in Figure 3) downward and artificially highlights the preseismic anomaly. Our analysis shows that the STEC increase relative to the blue cubic fit curve is an artifact of fitting to a STEC time series that includes an earthquake/tsunami-driven disturbance.

Several papers [see *Astafyeva et al.,* 2013; *Galvan et al.,* 2012; *Rolland et al.,* 2011; *Tsugawa et al.,* 2011] have reported perturbations in ionospheric TEC having large amplitude and exceptional time duration induced by the Tohoku-Oki main shock and/or to the generated tsunami. These perturbations last up to more than 2 h after the main shock. The exceptional time duration of the ionospheric perturbation is clearly evident in our STEC data as well (see Figures 2 and 3, black

curves). Our data show that on 11 March the STEC depletion starts at about 6:00 UT, just after the rapid increase that occurred 10 min after the earthquake, and lasts approximately 2 h. Therefore, since *Heki* [2011] in his analysis excludes only data in the period 5:12–6:00 UT, and *Heki and Enomoto* [2013] exclude data during the period −40 to +20 min from the earthquake time, their fitting procedure is clearly affected by the earthquake-related perturbations that are present in STEC data after 6:00 UT. In addition to that, by excluding data from 5:12 to 6:00 UT, *Heki* [2011] made an a priori decision regarding the occurrence time of the preseismic STEC anomaly, which means that this method cannot be used for earthquake prediction. Thus, we conclude that the cubic fit method adopted by *Heki* [2011] to identify preearthquake anomalies is unsatisfactory.

We emphasize that the primary focus of whether the preseismic STEC enhancement exists or not should be on the comparison with the STEC time series on surrounding days (Figure 2), rather than on the cubic fit analysis (Figure 3). Many of the fits shown in Figure 3 could be falsely interpreted as evidence of anomalous preseismic enhancement. However, Figure 2 shows that the flattening of the STEC time series is from natural ionospheric behavior and unrelated to earthquake. Typically, those who analyze TEC data use polynomial fitting methods only if there is no benchmark against which to compare the case of interest. This means that either data are not available for the same conditions on a different day or data are rendered unusable by other geophysical activity. In this case, as shown in Figure 2, the STEC time series on surrounding days are very much usable, and they show that the preseismic enhancement is normal.

To examine further whether the STEC enhancement prior to the earthquake is anomalous, we employ a statistical, Superposed Epoch Analysis of STEC curves from ± 30 days of the earthquake from GPS stations in Japan (GEONET 0035 and 0756), Mexico (lpaz), and Portugal (pdel). STEC curves are shifted in time such that maximum elevation angles for the satellites match. In other words, the curves are superposed epochs keyed to match when satellites were directly overhead. Figure 4 shows Superposed Epoch Analysis for GEONET GPS station 0756 in Japan and satellite 015. *Heki* [2011] presented STEC from the same station-satellite pair in his Figure 2 and reported that the enhancement starting about 40 min before the earthquake is a possible precursor. In Figure 4a, the black line is the day of the earthquake STEC, and the blue dots represent the mean of 61 curves from ± 30 days of the earthquake. The blue error bars are ± 1 standard deviation from the mean. Figure 4b shows residuals of cubic fits to the STEC curves in Figure 4a. The black line is the day of the earthquake residual STEC, and the blue dots represent the mean of 61 residual curves from ± 30 days of the earthquake. The blue error bars are ± 1 standard deviation from the mean residual. The red curve is the residual STEC from the earthquake day including only data prior to the earthquake time in the
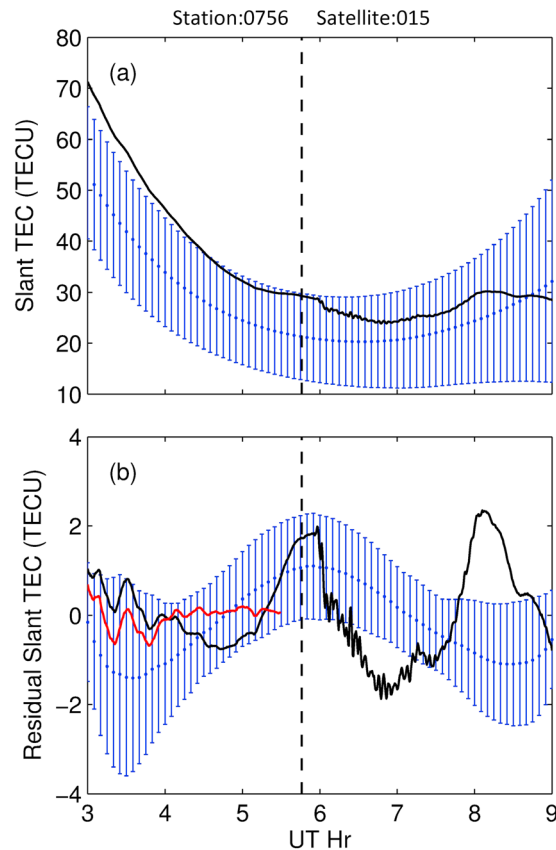
Figure 4. Superposed Epoch Analysis for GEONET GPS station 0756 in Japan and satellite 015. The time of the earthquake (5:46 UT) on 11 March is shown as the black vertical dashed line. (a) The black line is the day of the earthquake slant TEC, and the blue dots represent the mean of 61 curves from ± 30 days of the earthquake. The blue error bars are ± 1 standard deviation from the mean. (b) The black line is the day of the earthquake residual slant TEC, and the blue dots represent the mean of 61 residual curves from ± 30 days of the earthquake. The blue error bars are ± 1 standard deviation from the mean residual. The red curve is the residual slant TEC from the earthquake day including only data prior to the earthquake time in the cubic fit. See text for details.

cubic fit. The black curve uses the entire curve, including the earthquake-driven disturbance, for the cubic fit. Additional examples of STEC Superposed Epoch Analysis using other GPS stations and satellites in Japan, as well as stations in Mexico (lpaz) and Portugal (pdel), are shown in the supporting information. The stations in Mexico and Portugal show the STEC in regions far from Japan where earthquake-related signals should be minimal.

In the Superposed Epoch Analysis, we find that (i) the earthquake day STEC (and residuals) prior to the earthquake typical falls within ± 1 standard deviation of mean STEC for 60 days and always within ± 2 standard deviations; (ii) sometimes the residual shows an increase prior to the EQ and sometimes it does not, and increases are small, on the order of 1–2 TECU, which is approaching the uncertainty of the STEC values; and (iii) in agreement with our analysis of the fitting method shown in Figure 3, the residual STEC is dependent on whether data from after the earthquake time are included in the cubic fit, as seen by comparing the black and red curves in Figure 4b and in Figures S1–S6 in the supporting information. In summary, our statistical analysis shows that in any case, the reported STEC increase prior the earthquake was not particularly unusual and may be explained in terms of normal ionospheric variability.

3. The Magnitude Dependence of TEC Precursors

Taking into account our TEC analysis in section 2, we address the apparent earthquake magnitude dependence of the precursors reported by *Heki* [2011]. *Astafyeva et al.* [2013] demonstrated that stronger earthquakes generate TEC disturbances just after the main shock having longer-lasting depletion and larger amplitude. *Perevalova et al.* [2014] investigated GPS-TEC time series in correspondence of 38 earthquakes occurred from 1994 to 2012. They found a threshold (near M_w 6.5) of the magnitude below which postearthquakes ionospheric disturbances are difficult to detect. This threshold depends on geophysical conditions and on sensitivity of the GPS sounding method. These reports suggest that the amplitude of the ionospheric disturbances generated by earthquakes and tsunamis that may follow seaquakes [*Occhipinti et al.*, 2013] may be related to the magnitude and to the tectonic characteristics of the earthquakes.

With this perspective, the magnitude dependence of the precursors reported by *Heki* [2011, Figure 4b] can be easily explained. The preearthquake anomaly identified by *Heki* [2011] is relative to a cubic least squares fit of the STEC time series from 3:00 to 8:00 UT. Data from 5:12 to 6:00 UT were excluded in their fitting procedure as an attempt to remove the coseismic disturbance. However, disturbances after 6:00 UT are present in the TEC time series reported by *Heki* [2011] and *Heki and Enomoto* [2013], as well as in TEC data shown in our Figures 2 and 3. These disturbances are related to the earthquake and/or to the generated

tsunami [see *Kamogawa and Kakinami*, 2013; *Shinagawa et al.,* 2013]. As we have already discussed in section 2, STEC time series data from 6:00 to 8:00 UT influence the fitting procedure but were not excluded in fitting analysis of *Heki* [2011]. Since strong earthquakes trigger larger postseismic disturbances in ionospheric TEC [*Astafyeva et al.,* 2013], the fitting procedure adopted by *Heki* [2011] to extract the TEC anomaly is strongly influenced by the response of the ionosphere to the seismic disturbances. On the contrary the smaller TEC perturbations induced by less severe earthquakes have a negligible influence on the Heki's method. We conclude that the apparent earthquake magnitude dependence of the precursors reported by *Heki* [2011] is related to the amplitude of the postseismic ionospheric disturbances affecting the cubic fit to STEC time series data.

4. The 40 min Onset of TEC Precursors

Several possible physical mechanisms hypothesized to induce preearthquake seismogenic anomalies in the ionosphere have been proposed in scientific literature. They include the following: penetration in the ionosphere of atmospheric electric fields as a result of air ionization caused by radon emission from the Earth's crust; penetration in the ionosphere of electric fields generated by positively charged holes associated with microfracturing; and propagation up to the ionosphere of atmospheric gravity waves induced by thermal anomalies and others. Recently, these mechanisms have been unified in the Lithosphere-Atmosphere-Ionosphere Coupling model [see, e.g., *Pulinets and Ouzounov*, 2011]. However, in spite of the several published studies, as also pointed out by *Heki and Enomoto* [2013], the significance of these mechanisms has not yet been verified, and many researchers are skeptical of their reliability [see, e.g., *Denisenko et al.,* 2013; *Rishbeth*, 2006].

The main finding of *Heki and Enomoto* [2013] is the common onset of the reported VTEC anomalies about 40 min prior to four $M_w > 8$ strong earthquakes. The authors claim that these atmospheric disturbances have an intrinsic seismic origin, highlighting their exceptionally repeatability for strong earthquakes. The scenario proposed by *Heki and Enomoto* [2013] suggests that the TEC increase before each earthquake had a seismogenetic origin independent from tectonic context. We think that, in contrast, if this repeatability has seismic origin, it should be related to a geological and tectonic context which must be necessarily common to the areas where the earthquakes occur. Simply speaking, the scenario suggested by *Heki and Enomoto* [2013] requires that strong earthquakes occurred in different regions of the Earth were able to activate a mechanism, no matter what it is, that generated preearthquake TEC anomalies at the same lead time of 40 min. This statement has serious implications. If all $M_w > 8$ earthquakes shared the same precursory phase with a constant duration, they should also have had similar preparatory mechanisms, and as a consequence, they would display identical dynamic behavior and deformation pattern. This hypothesis is highly questionable, mainly because the earthquakes investigated by *Heki and Enomoto* [2013] had very inhomogeneous seismological properties and were generated in completely different tectonic and geodynamic scenarios. In our opinion the repeatability of the 40 min onsets does not support their conclusions. On the contrary, the simultaneous onset of the reported TEC anomalies is evidence that they are artifacts induced by the data fitting procedure. Here we briefly describe the four earthquakes investigated by *Heki and Enomoto* [2013] and summarize their main characteristics in Table 1.

4.1. Tohoku-Oki 2011 Earthquake

The M_w 9.0 2011 Tohoku-Oki interplate earthquake occurred offshore the east coast of Honshu (Japan), along the boundary between the Pacific and the Okhotsk plates. The rupture process lasted ~150 s, involving a 440–510 km long and 180–210 km wide fault segment dipping 13°, with 14.5 km hypocentral depth, 10 m averaged slip, and 48–50 m peak slip on the main patch [*Suzuki et al.,* 2011; *Yagi and Fukahata*, 2011]. It caused a devastating tsunami with a peak 40 m runup [*Romano et al.,* 2012]. This earthquake alone released most part of the strain accumulated for a quite long time interval in the subduction process of the Pacific plate (>80 mm/yr long-term rate). In fact, the only predecessor of the 2011 earthquake in the same area is the 869 A.D. event [*Minoura et al.,* 2001; *Scholz and Campos*, 2012; *Wang et al.,* 2012]. The main shock was preceded by >300 foreshocks, the largest of which (M_w 7.3) occurred 2 days before (9 March 2011, 2:45 UTC) with a focal mechanism consistent with that of the main shock [*Zhao et al.,* 2011].

Table 1. Seismological Parameters of the Four Earthquakes Investigated by *Heki and Enomoto* [2013][a]

Earthquake	Date/Origin Time (UTC)	Coordinates	M_w	Type	Hypocentral Depth (km)	Fault Dimensions (km²)	Fault Dip (°)	Average Slip (m)	Maximum Slip (m)	Rupture Duration (s)	Time Elapsed Since the Last Strongest Foreshock
Bengkulu	2007-09-12 11:10:26	4.517°S, 101.382°E	8.4	megathrust	30	~7×10⁴	12	3	>10	100	some centuries
Tohoku-Oki	2011-03-11 5:46:23	37.52°N, 143.05°E	9.0	megathrust	14.5	~1×10⁵	13	10	>50	150	~2 days (2011-03-09, M_w 7.3)
Sumatra	2012-04-11 8:38:37	2.327°N, 93.063°E	8.6	strike slip	22.9	~2×10⁴	74–85	7	37	120	~3 months (2012-01-11, M_w 7.2)
Sumatra	2012-04-11 10:43:09	0.802°N, 92.463°E	8.2	strike slip	25.1	na	subvertical	na	na	80	some centuries

[a]na, not available.

4.2. Bengkulu 2007 Earthquake

The Bengkulu M_w 8.4 interplate earthquake occurred offshore, near the west coast of Sumatra on 12 September 2007 (11:10:26 UTC). The rupture process lasted 100 s, involving a ~250–350 km long and 150–200 km wide fault segment dipping 12°, with 30 km hypocentral depth, 3 m averaged slip, and 6–12 m peak displacement on the main slip patch [*Konca et al.,* 2008; *Lorito et al.,* 2008; *Ambikapathy et al.,* 2010]. Despite the great magnitude, this earthquake triggered only a moderate tsunami (4 m runup) probably due to the intermediate depth of the main slip patch [*Lorito et al.,* 2008]. Importantly, this earthquake was not preceded by any documented foreshock activity because it involved a locked asperity, which probably had only partially ruptured during the catastrophic (*M*~9) event of 1833 [*Konca et al.,* 2008].

4.3. Sumatra 2012 Earthquakes

The North Sumatra intraplate M_w 8.6 earthquake (11 April 2012, 8:38:37 UTC) was the greatest strike-slip earthquake ever recorded in the instrumental era [*Pollitz et al.,* 2012; *Zhang et al.,* 2012]. Two hours later it was followed 185 km to the south-southwest by a M_w 8.2 aftershock, with a similar focal mechanism. The largest foreshock (M_w 7.2) occurred 3 months before on 10 January 2012. These two great earthquakes share some very unusual features: (1) no tsunami was triggered, (2) they were of intraplate type (Wharton Basin) [*Deplus et al.,* 1998], and (3) they had an extremely complex rupture history. The M_w 8.6 earthquake rupture process lasted 120 s, involving three segments of a conjugate strike-slip fault system for a total length of about 470 km, with 7 m averaged slip and 37 m peak slip on the main patch [*Yue et al.,* 2012; *Zhang et al.,* 2012]. The M_w 8.2 aftershock was dynamically triggered by the main shock [*Pollitz et al.,* 2012], whereas its rupture lasted about 80 s [*Yue et al.,* 2012].

The four aforementioned earthquakes belong to two main groups: interplate and intraplate types. The only similarity between the 2011 Tohoku-Oki and the 2007 Bengkulu interplate earthquakes is that they originated at the interface between one subducting plate (the Pacific and the Australian plates, respectively) and an overriding plate (the Okhotsk and the Indian plates, respectively). On the other hand, they are completely different in terms of fault dimensions, rupture duration, complexity, and associated slip. The background geodynamic scenario also differs in both cases. In the Japanese area, in fact, the long-term subduction rate of the Pacific plate is 75–94 mm/yr (83 mm/yr in the Honshu sector) [*Scholz and Campos,* 2012], whereas the long-term convergence rate of the Australian plate at the Sunda trench is 25 mm/yr [*Bird et al.,* 2008] to 45 mm/yr [*Scholz and Campos,* 2012]. The seismic coupling [*McCaffrey,* 1997] of the two subduction zones also differs, being on the order of 0.5 for the Honshu trench and ~1 for the Sumatra trench [*Scholz and Campos,* 2012]. This testifies for completely different seismotectonic behaviors:

the Sumatra subduction zone features more highly coupled patches with respect to the Japanese one. Any possible similarity in the preparatory phase of these giant megathrust earthquakes seems therefore unlikely.

With regard to the two 2012 North Sumatra earthquakes, they had the similar focal mechanism; nevertheless, they had extremely different slip history and rupture pattern. Moreover, since the M_w 8.2 earthquake was the first aftershock of the M_w 8.6 main shock, the ~2 h lag between the two events have no physical relation with the presumed ~40 min preevent rise of TEC. Moreover, the largest foreshock of the M_w 8.6 event occurred 3 months before: while there is little doubt on the influence of this foreshock in critically perturbing the stress field surrounding the source of the main shock, the 3 months time interval has no relation with the presumed 40 min lead time preceding the 11 April earthquake. The same is true for the 2011 Tohoku-Oki earthquake, whose largest foreshock occurred 2 days before. The Bengkulu 2007 earthquake, finally, was not preceded by any foreshock.

In summary, the only characteristic that is common to the four earthquakes is that their magnitude was larger than M_w 8.0. However, this does not mean that the earthquakes were similar, nor it can justify the repeatability of the onset of preseismic TEC anomalies 40 min before main shocks.

5. Were Tohoku-Oki Precursory Signals Detected by Other Sensors?

Heki and Enomoto [2013] investigated also magnetic and ionosonde data at the time the Tohoku-Oki 2011 earthquake. They analyzed data from the ionosonde of Kokubunji (35.71°N, 139.49°E), west of Tokyo and reported an increase of the sporadic E layer critical frequency f_oE_s before the Tohoku-Oki main shock. The f_oE_s increase seems to be almost coincident with the VTEC increase [see *Heki and Enomoto*, 2013, Figure 4]. A more detailed discussion of the f_oE_s increase before the Tohoku earthquake can be found in *Carter et al.* [2013]. They reported a statistical investigation of the occurrence of similar f_oE_s increases in 6 years (2006–2011) of data from the Japanese ionosondes of Wakkanai (45.16°N, 141.75°E), Kokubunji, and Yamagawa (31.20°N, 130.62°E). According to *Carter et al.* [2013], the f_oE_s anomaly reported by *Heki and Enomoto* [2013] prior to the Tohoku-Oki earthquake is not unique, since similar increases have been observed in Japan many more times without a corresponding seismic activity. They also pointed out that the f_oE_s increase may have been induced by the high geomagnetic activity that peaked in intensity on 11 March just 21 min before the Tohoku-Oki main shock [see *Carter et al.,* 2013, Figure 2].

Heki and Enomoto [2013] analyzed magnetic data from six Japanese stations. Geomagnetic field components time series of each station are shown relative to the components of Kanoya (31.42°N, 130.88°E), the farthest station from the earthquake area, which was chosen as reference by the authors. According to *Heki and Enomoto* [2013], the four stations closest to the epicenter showed anomalies in the magnetic declination that seem to be coincident with the VTEC anomaly on 11 March [see *Heki and Enomoto*, 2013, Figure 4]. On the contrary, no corresponding anomaly seems to be present in the other geomagnetic field components. In Figure 5, we show the geomagnetic field components of Kakioka (36.23°N, 140.12°E) relative to Kanoya as reported in the supporting information (Figure A3) of *Heki and Enomoto* [2013]. We note that the geomagnetic observatory of Kakioka is away from Kanoya, about 1000 km. Due to the large distance between the two stations, we are skeptical that global magnetic disturbances may have been removed from Kakioka data by the simple differentiation method adopted by the authors. Figure 5 shows that magnetic disturbances, which seem to be almost coincident with CID presents in VTEC time series, started a few minutes after the 11 March main 2009shock and, contrary to the magnetic precursor reported by *Heki and Enomoto* [2013], are present in all the components of the geomagnetic field. Then, after about 10 min from the earthquake, each component shows a rapid decrease followed by a slow recovery to normal values. The common behavior of the geomagnetic field components after the Tohoku-Oki earthquake suggests that the postseismic magnetic disturbances were probably generated by electric currents induced in the ionosphere by the arrival of atmospheric waves excited by the earthquake and the generated tsunami. Similar postseismic magnetic disturbances were also found by *Kherani et al.* [2012] and *Utada et al.* [2011] during a few minutes after the Tohoku-Oki main shock. According to *Heki and Enomoto* [2013], the presence of the preearthquake anomaly only in the declination suggests that the disturbed magnetic field was dominantly (i.e., almost polarized) in the east-west direction. In our opinion, it is very hard to accept that this scenario is realistic. What is the physical mechanism that generated the polarized
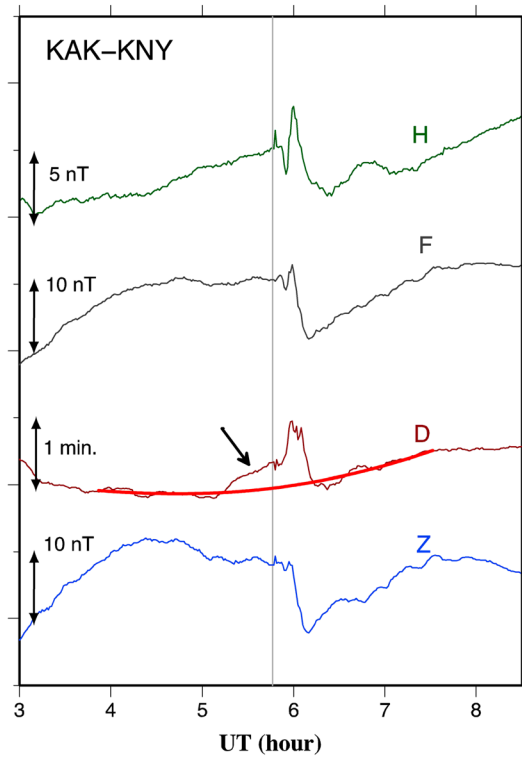
Figure 5. Horizontal component *H*, total field *F*, declination *D*, and the vertical component *Z* of the geomagnetic field of Kakioka (KAK: 36.23°N, 140.12°E) relative to Kanoya (KNY: 31.42°N, 130.88°E) during the hours before and after the Tohoku earthquake as reported in the supporting information (Figure A3) of *Heki and Enomoto* [2013]. The time of the earthquake (5:46 UT) on 11 March is shown as grey vertical line. The black arrow indicates the possible seismogenic increase that is present only in the declination. The red curve has been added to the original view to show the fitting procedure adopted to extract the preearthquake anomaly [see *Heki and Enomoto*, 2013, Figure 4].

magnetic disturbance? Note that the method used by *Heki and Enomoto* [2013] to extract the declination anomaly is similar to that they adopted for TEC time series. Thus, we think that, as for STEC and VTEC, the anomaly in the declination is due to the baseline assumed in the fitting procedure (red curve in Figure 5) [see *Heki and Enomoto*, 2013, Figure 4]. Something that can also be seen from Figure 5 is that *Heki and Enomoto* [2013] found an anomaly only in the declination since a similar fitting procedure cannot be adopted for the other geomagnetic field components. In addition to that, as we have already reported, it should be noted that the Tohoku-Oki earthquake occurred during a magnetically disturbed period [see *Heki and Enomoto*, 2013, Figure 6a] that could have driven disturbances both in ionospheric TEC and geomagnetic field components.

In a recent report, *Utada and Shimizu* [2014] have investigated the spatial dependence of the geomagnetic declination over Japan at the time of the Tohoku-Oki earthquake. They have found a large declination change after the earthquake in geomagnetic data from stations closest to the epicentral area (latitude range of 35–40°N). On the contrary, according to them, the declination change that preceded the Tohoku-Oki earthquake shows a linear dependence with latitude in a larger latitude range (25–45°N) without showing any significant feature in the epicentral region. *Utada and Shimizu* [2014] concluded that the large spatial scale shown by the preseismic declination change suggests that it had external origin like storm-time disturbances. Conversely, the postseismic declination change that is almost localized in the epicentral region may be associated to the earthquake and the generated tsunami. Thus, the study by *Utada and Shimizu* [2014] lends support to our findings. Namely, the preseismic declination change reported by *Heki and Enomoto* [2013] at Kakioka is an artifact induced by the assumed baseline (red curve in Figure 5). In conclusion, the declination change, as well as the f_oE_s increase, that they have reported does not support the seismogenic origin of the preearthquake TEC enhancement.

6. Conclusions

We have examined the reports of *Heki* [2011] and *Heki and Enomoto* [2013]. We have shown that the STEC enhancement reported by *Heki* [2011] before the 2011 Tohoku-Oki earthquake is not really anomalous; instead, it is in artifact of curve fitting to data that includes postseismic disturbances induced by the earthquake and the generated tsunami. TEC time series prior to the Tohoku-Oki earthquake appear to record essentially normal global-scale variation, which is supported by a Superposed Epoch Analysis using STEC curves from ± 30 days of the earthquake. We cast serious doubt on the reliability of the scenario proposed by *Heki and Enomoto* [2013] regarding the simultaneous onset of VTEC increases ~40 min before the occurrence of strong earthquakes. This scenario should necessarily imply that the generation mechanism of these

anomalies should be common in the four earthquakes studied. More importantly, this mechanism would need to be activated with the same lead time of 40 min. In our opinion, this scenario is not supported by the tectonic and geodynamic characteristics of the four earthquakes. In addition to that, further analyses reported by *Heki and Enomoto* [2013] using ionosonde and geomagnetic data do not show strong evidence of corresponding preseismic anomalies that might be associated to the 11 March 2011 Tohoku-Oki earthquake. We conclude that the TEC increases documented by *Heki* [2011] and *Heki and Enomoto* [2013] just before $M_w > 8$ earthquakes cannot be uniquely associated with the seismic activity. Thus, we find no evidence to support the hypothesis that TEC anomalies like these can be used to predict times, locations, and magnitudes of pending earthquakes.

References

Afraimovich, E. L., and E. I. Astafyeva (2008), TEC anomalies-local TEC changes prior to earthquakes or TEC response to solar activity changes?, *Earth Planets Space*, *60*, 961–966.

Ambikapathy, A., J. K. Catherine, V. K. Gahalaut, M. Narsaiah, A. Bansal, and P. Mahesh (2010), The 2007 Bengkulu earthquake, its rupture model and implications for seismic hazard, *J. Earth Syst. Sci.*, *119*(4), 553–560, doi:10.1007/s12040-010-0037-2.

Astafyeva, E., and K. Heki (2011), Vertical TEC over seismically active region during low solar activity, *J. Atmos. Sol. Terr. Phys.*, *73*(13), 1643–1652, doi:10.1016/j.jastp.2011.02.020.

Astafyeva, E., P. Lognonné, and L. Rolland (2011), First ionospheric images of the seismic fault slip on the example of the Tohoku-Oki earthquake, *Geophys. Res. Lett.*, *38*, L22104, doi:10.1029/2011GL049623.

Astafyeva, E., S. Shalimov, E. Olshanskaya, and P. Lognonné (2013), Ionospheric response to earthquakes of different magnitudes: Larger quakes perturb the ionosphere stronger and longer, *Geophys. Res. Lett.*, *40*, 1675–1681, doi:10.1002/grl.50398.

Bird, P., Z. Liu, and W. K. Rucker (2008), Stresses at the plates from below: Definitions, computational path, model optimization, and error analysis, *J. Geophys. Res.*, *113*, B11406, doi:10.1029/2007JB005460.

Bishop, G., D. Walsh, P. Daly, A. Mazzella, and E. Holland (1994), Analysis of temporal stability of GPS and GLONASS group delay correction terms seen in various sets of ionospheric delay data, in *Proceedings of ION GPS-94*, pp. 1653–1661, The Institute of Navigation, Washington, D. C.

Cahyadi, M. N., and K. Heki (2013), Ionospheric disturbances of the 2007 Bengkulu and the 2005 Nias earthquakes, Sumatra, observed with a regional GPS network, *J. Geophys. Res. Space Physics*, *118*, 1777–1787, doi:10.1002/jgra.50208.

Calais, E., and J. B. Minster (1995), GPS detection of ionospheric perturbations following the January 17, 1994, Northridge earthquake, *Geophys. Res. Lett.*, *22*, 1045–1048, doi:10.1029/95GL00168.

Campbell, W. H. (2009), Natural magnetic disturbance fields, not precursors, preceding the Loma Prieta earthquake, *J. Geophys. Res.*, *114*, A05307, doi:10.1029/2008JA013932.

Carter, B. A., A. C. Kellerman, T. A. Kane, P. L. Dyson, R. Norman, and K. Zhang (2013), Ionospheric precursors to large earthquakes: A case study of the 2011 Japanese Tohoku Earthquake, *J. Atmos. Sol. Terr. Phys.*, *102*, 290–297, doi:10.1016/j.jastp.2013.06.006.

Dautermann, T., E. Calais, J. Haase, and J. Garrison (2007), Investigation of ionospheric electron content variations before earthquakes in southern California, 2003–2004, *J. Geophys. Res.*, *112*, B02106, doi:10.1029/2006JB004447.

Denisenko, V. V., M. Ampferer, E. V. Pomozov, A. V. Kitaev, W. Hausleitner, G. Stangl, and H. K. Biernat (2013), On electric field penetration from ground into the ionosphere, *J. Atmos. Sol. Terr. Phys.*, *102*, 341–353, doi:10.1016/j.jastp.2013.05.019.

Deplus, C., M. Diament, H. Hebert, G. Bertrand, S. Dominguez, J. Dubois, J. Malod, P. Patriat, B. Pontoise, and J. Sibilla (1998), Direct evidence of active deformation in the eastern Indian oceanic plate, *Geology*, *26*, 131–134, doi:10.1130/0091-7613(1998)026<0131:DEOADI>2.3.CO;2.

Galvan, D. A., A. Komjathy, M. P. Hickey, P. Stephens, J. Snively, Y. Tony Song, M. D. Butala, and A. J. Mannucci (2012), Ionospheric signatures of Tohoku-Oki tsunami of March 11, 2011: Model comparisons near the epicenter, *Radio Sci.*, *47*, RS4003, doi:10.1029/2012RS005023.

Hao, Y. Q., Z. Xiao, and D. H. Zhang (2012), Multi-instrument observation on co-seismic ionospheric effects after great Tohoku earthquake, *J. Geophys. Res.*, *117*, A02305, doi:10.1029/2011JA017036.

Hao, Y. Q., Z. Xiao, and D. H. Zhang (2013), Teleseismic magnetic effects (TMDs) of 2011 Tohoku earthquake, *J. Geophys. Res. Space Physics*, *118*, 3914–3923, doi:10.1002/jgra.50326.

Heki, K. (2011), Ionospheric electron enhancement preceding the 2011 Tohoku-Oki earthquake, *Geophys. Res. Lett.*, *38*, L17312, doi:10.1029/2011GL047908.

Heki, K., and Y. Enomoto (2013), Preseismic ionospheric electron enhancements revisited, *J. Geophys. Res. Space Physics*, *118*, 6618–6626, doi:10.1002/jgra.50578.

Kajitani, Y., S. E. Chang, and H. Tatano (2013), Economic impacts of the 2011 Tohoku-Oki earthquake and tsunami, *Earthquake Spectra*, *29*(S1), S457–S478, doi:10.1193/1.4000108.

Kakinami, Y., M. Kamogawa, Y. Tanioka, S. Watanabe, A. R. Gusman, J.-Y. Liu, Y. Watanabe, and T. Mogi (2012), Tsunamigenic ionospheric hole, *Geophys. Res. Lett.*, *39*, L00G27, doi:10.1029/2011GL050159.

Kamogawa, M., and Y. Kakinami (2013), Is an ionospheric electron enhancement preceding the 2011 Tohoku-Oki earthquake a precursor?, *J. Geophys. Res. Space Physics*, *118*, 1751–1754, doi:10.1002/jgra.50118.

Kherani, E. A., P. Lognonné, H. Hébert, L. Rolland, E. Astafyeva, G. Occhipinti, P. Coïsson, D. Walwer, and E. R. de Paula (2012), Modelling of the total electronic content and magnetic field anomalies generated by the 2011 Tohoku-Oki tsunami and associated acoustic gravity waves, *Geophys. J. Int.*, doi:10.1111/j.1365-246X.2012.05617.x.

Konca, A. O., et al. (2008), Partial rupture of a locked patch of the Sumatra megathrust during the 2007 earthquake sequence, *Nature*, *456*, 631–635, doi:10.1038/nature07572.

Le, H., J. Y. Liu, and L. Liu (2011), A statistical study of ionospheric anomalies before 736 M6.0+ earthquakes during 2002–2010, *J. Geophys. Res.*, *116*, A02303, doi:10.1029/2010JA015781.

Le, H., L. Liu, J.-Y. Liu, B. Zhao, Y. Chen, and W. Wan (2013), The ionospheric anomalies prior to the M9.0 Tohoku-Oki earthquake, *J. Asian Earth Sci.*, *62*, 476–484, doi:10.1016/j.jseaes.2012.10.034.

Lorito, S., F. Romano, A. Piatanesi, and E. Boschi (2008), Source process of the September 12, 2007, M_w 8.4 southern Sumatra earthquake from tsunami tide gauge record inversion, *Geophys. Res. Lett.*, *35*, L02310, doi:10.1029/2007GL032661.

Maruyama, T., and H. Shinagawa (2014), Infrasonic sounds excited by seismic waves of the 2011 Tohoku-oki earthquake as visualized in ionograms, *J. Geophys. Res. Space Physics*, *119*, 4094–4108, doi:10.1002/2013JA019707.

Masci, F. (2010), On claimed ULF seismogenic fractal signatures in the geomagnetic field, *J. Geophys. Res.*, *115*, A10236, doi:10.1029/2010JA015311.

Masci, F. (2011), On the seismogenic increase of the ratio of the ULF geomagnetic field components, *Phys. Earth Planet. Inter.*, *187*, 19–32, doi:10.1016/j.pepi.2011.05.001.

Masci, F. (2012), The study of ionospheric anomalies in Japan area during 1998–2010 by Kon et al.: An inaccurate claim of earthquake-related signatures?, *J. Asian Earth Sci.*, *57*, 1–5, doi:10.1016/j.jseaes.2012.06.009.

Masci, F. (2013), Further comments on the ionospheric precursor of the 1999 Hector Mine earthquake, *Nat. Hazards Earth Syst. Sci.*, *13*, 193–196, doi:10.5194/nhess-13-193-2013.

Masci, F., and J. N. Thomas (2014), Comment on "Temporal and spatial precursors in ionospheric total electron content of the 16 October 1999 M_w 7.1 Hector Mine earthquake" by Su et al. (2013), *J. Geophys. Res. Space Physics*, *119*, 6994–6997, doi:10.1002/2014JA019896.

Mazzella, A. J., G. S. Rao, G. J. Bailey, G. J. Bishop, and L. C. Tsai (2007), GPS determinations of plasmasphere TEC, in *Proceedings of the International Beacon Satellite Symposium 2007*, edited by P. Doherty, Boston College, Boston, Mass.

McCaffrey, R. (1997), Statistical significance of the seismic coupling coefficient, *Bull. Seismol. Soc. Am.*, *87*, 1069–1073.

Minoura, K., F. Imamura, D. Sugawara, Y. Kono, and T. Iwashita (2001), The 869 Jogan tsunami deposit and recurrence interval of large-scale tsunami on the Pacific coast of northeast Japan, *J. Nat. Disaster Sci.*, *23*, 83–88.

Moldovan, I. A., A. O. Placinta, A. P. Constantin, A. S. Moldovan, and C. Ionescu (2012), Correlation of geomagnetic anomalies recorded at Muntele Rosu Seismic Observatory (Romania) with earthquake occurrence and solar magnetic storms, *Ann Geophys-Italy*, *55*(1), 125–137, doi:10.4401/ag-5367.

Occhipinti, G., L. Rolland, P. Lognonné, and S. Watada (2013), From Sumatra 2004 to Tohoku-Oki 2011: The systematic GPS detection of the ionospheric signature induced by tsunamigenic earthquakes, *J. Geophys. Res. Space Physics*, *118*, 3626–3636, doi:10.1002/jgra.50322.

Perevalova, N. P., V. A. Sankov, E. I. Astafyeva, and A. S. Zhupitayaeva (2014), Threshold magnitude for ionospheric TEC response to earthquake, *J. Atmos. Sol. Terr. Phys.*, *108*, 77–90, doi:10.1016/j.jastp.2013.12.014.

Pollitz, F., R. S. Stein, V. Sevilgen, and R. Burgmann (2012), The 11 April 2012 east Indian Ocean earthquake triggered large aftershocks worldwide, *Nature*, *490*, 250–253, doi:10.1038/nature11504.

Pulinets, S., and D. Ouzounov (2011), Lithosphere–Atmosphere–Ionosphere Coupling (LAIC) model—An unified concept for earthquake precursors validation, *J. Asian Earth Sci.*, *41*, 371–382, doi:10.1016/j.jseaes.2010.03.005.

Rishbeth, H. (2006), Ionoquakes: Earthquake precursors in the ionosphere?, *Eos Trans. AGU*, *87*(32), 316, doi:10.1029/2006EO320008.

Rolland, L., P. Lognonne, E. Astafyeva, A. Kherani, N. Kobayashi, M. Mann, and H. Munekane (2011), The resonant response of the ionosphere imaged after the 2011 Tohoku-Oki earthquake, *Earth Planets Space*, *63*(7), 853–857, doi:10.5047/eps.2011.06.020.

Romano, F., A. Piatanesi, S. Lorito, N. D'Agostino, K. Hirata, S. Atzori, Y. Yamazaki, and M. Cocco (2012), Clues from joint inversion of tsunami and geodetic data of the 2011 Tohoku-Oki earthquake, *Sci. Rep.*, *2*, 385, doi:10.1038/srep00385.

Scholz, C. H., and J. Campos (2012), The seismic coupling of subduction zones revisited, *J. Geophys. Res.*, *117*, B05310, doi:10.1029/2011JB009003.

Shinagawa, H., T. Tsugawa, M. Matsumura, T. Iyemori, A. Saito, T. Maruyama, H. Jin, M. Nishioka, and Y. Otsuka (2013), Two-dimensional simulation of ionospheric variations in the vicinity of the epicenter of the Tohoku-Oki earthquake on 11 March 2011, *Geophys. Res. Lett.*, *40*, 5009–5013, doi:10.1002/2013GL057627.

Suzuki, W., S. Aoi, H. Sekiguchi, and T. Kunugi (2011), Rupture process of the 2011 Tohoku-Oki mega-thrust earthquake (M9.0) inverted from strong motion data, *Geophys. Res. Lett.*, *38*, L00G16, doi:10.1029/2011GL049136.

Thomas, J. N., J. J. Love, and M. J. S. Johnston (2009a), On the reported magnetic precursor of the 1989 Loma Prieta earthquakes, *Phys. Earth Planet. Inter.*, *173*, 207–215, doi:10.1016/j.pepi.2008.11.014.

Thomas, J. N., J. J. Love, M. J. S. Johnston, and K. Yumoto (2009b), On the reported magnetic precursor of the 1993 Guam earthquake, *Geophys. Res. Lett.*, *36*, L16301, doi:10.1029/2009GL039020.

Thomas, J. N., J. J. Love, A. Komjathy, O. P. Verkhoglyadova, M. Butala, and N. Rivera (2012a), On the reported ionospheric precursor of the 1999 Hector Mine, California earthquake, *Geophys. Res. Lett.*, *39*, L06302, doi:10.1029/2012GL051022.

Thomas, J. N., F. Masci, J. J. Love, and M. J. S. Johnston (2012b), Reported geomagnetic and ionospheric precursors to earthquakes: Summary, reanalysis, and implication for short-term prediction, paper presented at AGU Fall Meeting, San Francisco, Calif., 3–7 Dec.

Tsugawa, T., A. Saito, Y. Otsuka, M. Nishioka, T. Maruyama, H. Kato, T. Nagatsuma, and K. T. Murata (2011), Ionospheric disturbances detected by GPS total electron content observation after the 2011 off the Pacific coast of Tohoku Earthquake, *Earth Planets Space*, *63*, 875–879, doi:10.5047/eps.2011.06.035.

Utada, H., and H. Shimizu (2014), Comment on "Preseismic ionospheric electron enhancements revisited" by K. Heki and Y. Enomoto, *J. Geophys. Res. Space Physics*, *119*, 6011–6015, doi:10.1002/2014JA020044.

Utada, H., H. Shimizu, T. Ogawa, T. Maeda, T. Furumura, T. Yamamoto, N. Yamazaki, Y. Yoshitake, and S. Nagamachi (2011), Geomagnetic field changes in response to the 2011 off the Pacific Coast of Tohoku earthquake and tsunami, *Earth Planet. Sci. Lett.*, *311*, 11–27, doi:10.1016/j.epsl.2011.09.036.

Wang, L., C. K. Shum, F. J. Simons, B. Tapley, and C. Dai (2012), Coseismic and postseismic deformation of the 2011 Tohoku-Oki earthquake constrained by GRACE gravimetry, *Geophys. Res. Lett.*, *39*, L07301, doi:10.1029/2012GL051104.

Yagi, Y., and Y. Fukahata (2011), Rupture process of the 2011 Tohoku-Oki earthquake and absolute elastic strain release, *Geophys. Res. Lett.*, *38*, L19307, doi:10.1029/2011GL048701.

Yue, H., T. Lay, and K. D. Koper (2012), En echelon and orthogonal fault ruptures of the 11 April 2012 great intraplate earthquake, *Nature*, *490*, 245–249, doi:10.1038/nature11492.

Zhang, H., J. Chen, and Z. Ge (2012), Multi-fault rupture and successive triggering during the 2012 M_w 8.6 Sumatra offshore earthquake, *Geophys. Res. Lett.*, *39*, L22305, doi:10.1029/2012GL053805.

Zhao, D., Z. Huang, N. Umino, A. Hasegawa, and H. Kanamori (2011), Structural heterogeneity in the megathrust zone and mechanism of the 2011 Tohoku-oki earthquake (M_w 9.0), *Geophys. Res. Lett.*, *38*, L17308, doi:10.1029/2011GL048408.